55.0 FE-CONTAINING MULTI-PRINCIPAL ELEMENT ALLOYS FOR PROTECTIVE STRUCTURES

James Frishkoff (Mines)
Faculty: Amy Clarke and Kester Clarke (Mines)
Industrial Mentor: Bruce Antolovich (ATI), Hayley Brown (SFSA), Steve Jansto (CBMM), Tanya Ros (Arcelor Mittal)

This project initiated in Spring 2021 and is supported by Steel Founders Society of America and the Steel Performance Initiative. The research performed during this project will serve as the basis for an M.S. thesis program for James Frishkoff.

55.1 Project Overview and Industrial Relevance

Multi-principal element alloys (MPEAs), also referred to as high-entropy alloys (HEAs) or complex concentrated alloys (CCAs), are a new class of alloys defined by the presence of four or more major alloying elements, in equiatomic or near-equiatomic ratio, as shown in **Figure 55.1** [55.1]. A development of interest within the MPEA design space is metastable, dual-phase multi-principal element alloys (DP-MPEAs), which have demonstrated significant tensile strength – ductility combinations and high work-hardening rates enabled by composition- and processing-tunable transformation-induced plasticity (TRIP) and twinning-induced plasticity (TWIP) [55.2]. These property combinations are attractive for blast- and ballistic impact resistance settings, including armored vehicle structures. [55.3] The majority of metastable MPEAs reported in the literature contain 10 at.% or more cobalt. Cobalt is an expensive raw element, a worker safety hazard, and an environmental contamination risk, all of which act as industrial cost drivers. This project focuses on the development of new cobalt-free metastable MPEA compositions via a literature-guided and thermodynamic modeling approach.

Most of the mechanical properties reported thus far for metastable DP-MPEAs are under conditions of uniaxial tension, quasi-static strain rate, and room temperature. Ballistic and blast loading conditions impose strain rates of 10^2-10^3 s^{-1} and transient plastic heating up to 1000K [55.4]. In addition, knowledge of the mechanical response at elevated temperatures and strain rates is important for developing processing maps. This project will therefore incorporate tests in a Gleeble® thermomechanical processing simulator. The data from these tests will then be used to calculate coefficients and exponents for the Johnson-Cook and Zerilli Armstrong constitutive models. Constitutive models are useful for comparing the mechanical properties of different alloys at elevated temperatures and strain rates .

55.2 Previous Work

This project builds upon a thermodynamic modeling methodology developed during a previous CANFSA student's M.S. thesis. John Copley's thesis focused on the TRIP effect in the CoCrNi MPEA alloy space, but in the course of his project he validated a computational method for predicting TRIP behavior in ferrous alloys. For alloys which undergo a martensitic transformation there exists a temperature called the diffusionless transformation temperature (T_0), indicating the temperature at which the austenite and martensite phases have the same Gibbs energy. The T_0 is the highest temperature where a martensite phase can form. Copley showed that if the ambient temperature divided by T_0 is less than 1, the alloy likely exhibits TRIP behavior. [55.5] The T_0 temperature is easily calculated in commercial thermodynamic modeling software, including Thermo-Calc. The T_0 temperature is therefore used in this project as a screening parameter.

This project also incorporates the work of another CANFSA alum, Francisco Coury. Coury developed a computational model for predicting the solid solution strengthening contribution in MPEAs called TC-EARS. [55.6] This model provides a second screening parameter for alloy design. The use of this parameter is discussed further in Section 55.3.2.

55.3 Recent Progress

55.3.1 Thermodynamic Screening

Thermo-Calc is a thermodynamic modeling software package that allows for the calculation of phase diagrams, precipitation kinetics, and thermophysical and thermochemical properties. The Thermo-Calc screening in this project focuses on several performance metrics. The composition constraints are the first metric. The composition space is limited to the 3*d* transition metals, as well as Mo, W, Nb Al, Si, N, B, and C. Co is excluded and Fe is preferred as the dominant element, while maintaining compositional criteria for consideration as an MPEA. Dual-phase equilibrium microstructures are preferred, as they are associated with lower critical strain for TRIP initiation [55.7]. The formation of brittle intermetallic phases, such as σ phase upon heat treating, is not automatically disqualifying, as the formation kinetics are likely slow. However, the prediction of more than 5 vol.% brittle intermetallics at room temperature is considered disqualifying. An elevated-temperature brittle-phase field that substantially overlaps the phase fields for desirable precipitates is also a rejection criterion, as it will likely cause problems heat treating precipitation-hardened alloys to a peak age condition. γ' (L_{12} ordered FCC phase) precipitates have been the focus of most precipitation-hardening alloy design in this project, as they are known to exist in a number of MPEA chemistry ranges and have previously been shown to improve the ballistic properties of TRIP steels [55.8, 55.9]. The screening process has also assessed other precipitate families, including TiB_2 and an Fe_2SiTi precipitate, which was recently described in a FeNiCoMnTiSi MPEA. [55.10] However, no Co-free and brittle-phase-free chemistries have been identified thus far with these precipitates.

The precipitation simulation mode in Thermo-Calc was used in this project to attempt to screen for chemistries which could be easily heat treated to a high volume fraction of precipitates in the peak aged condition. Simulations of selected γ'-producing chemistries indicate very slow precipitation kinetics. A representative isothermal transformation curve is given in **Figure 55.2**. Several papers describe much faster γ' precipitation kinetics in experimental heat treatments, so further experimentation is necessary to determine if kinetic parameters in current Thermo-Calc databases are accurate. [55.8]

Thermo-Calc was also used to assess alloy metastability, both via free energy curves and diffusionless transformation temperature (T_0) calculations. This is a continuation of the approach developed by Copley et al. [55.5] Once a candidate composition was identified through the equilibrium phase diagram, free energy curves for the FCC and BCC phases were extracted from Thermo-Calc. The equilibrium composition of the FCC phase was then taken as the input for the built-in T_0 algorithm in Thermo-Calc. The FCC phase is taken as the parent phase, because in the majority of experimentally observed TRIP MPEAs, the FCC phase is the parent phase for the martensite transformation. Several Co-free compositions with favorable T_0 values have been identified through this approach so far, as shown in **Figure 55.3**.

This project has identified one significant barrier to the utility of thermodynamic modeling as a screening tool for MPEA design. Current Thermo-Calc databases (TC-HEA4 and TC-FE11) do not account for the experimentally-observed hexagonal close-packed phase in $Fe_{50}Mn_{30}$ – derived compositions. Further work is needed to determine if this should be resolved in future database editions, or if in fact the HCP phase in this composition space is itself metastable rather than stable. This is outside the scope of the current project, however. Cross-examination in PanDAT, a similar CALPHAD software produced by CompuTherm LLC, also does not predict an HCP phase in this system. The current inability of CALPHAD software to predict experimentally-observed phase transformations poses the risk that this project is excluding compositions which could have desirable property combinations.

To attempt to close this gap, estimates of the intrinsic stacking fault energy were made. The stacking fault energy correlates to phase stability as well as different deformation mechanisms, as shown in **Figure 55.4**. [55.11] A modified Olson-Cohen thermodynamic method was adapted from the TRIP/TWIP steels literature. [55.12] This method produced the results shown in **Figure 55.3**. However, it is not known whether this method is accurate for highly alloyed materials like MPEAs. It is also compositionally limited, as it only provides coefficients for Mn, Cr, Ni, Cu, Al, Si, Fe, and C. The majority of the MPEA literature uses density functional theory (DFT) algorithms and high-performance computing clusters to calculate stacking fault energies. This method was not selected for the current project to avoid scope creep.

55.3.2 TC-EARS Solid Solution Strengthening Screening

Solid solution strength contributions of candidate alloys were calculated using the Toda-Carabello – Effective Atomic Radii for Strength (TC-EARS) model developed in [55.6]. For calculating the overall solid solution strength contribution in dual-phase alloys, the equilibrium chemistry and volume fraction for each phase was extracted from Thermo-Calc and fed into the TC-EARS algorithm. The specific strengthening contributions for each phase were then weighted according to the volume fraction to produce a bulk solid solution strengthening term. The specific strengths of each phase were also recorded, in order to predict which phase would yield first. TC-EARS strengthening results for six candidate compositions are given in **Figure 55.3**.

55.3.3 Baseline Material for Comparison

Three industrially-produced alloys have been sourced from ATI Specialty Materials. These alloys will provide baseline mechanical and microstructural evolution information against which the new MPEAs will be measured. These alloys are ATI 188, a cobalt-base high temperature alloy with a high work hardening rate suggestive of TRIP behavior; A286, a well-characterized NiCr steel which also exhibits TRIP behavior; and Datalloy HP, an austenitic alloy developed by ATI which approaches the composition ranges of some MPEAs. Vacuum-processed ingots of these alloys have been received at Colorado School of Mines and have been sent out for machining.

55.3.4 Mechanical Test Methodology

A mechanical test plan has been developed for the next stage of this project. It consists of room-temperature tensile tests at three different strain rates, Gleeble tensile tests at two different elevated temperatures and three strain rates, and Gleeble compression tests at three temperatures and strain rates. The test matrices are given as **Figure 55.5** and **Figure 55.6**. The tensile tests will provide data for fitting to Johnson-Cook and Zerilli-Armstrong constitutive models, while the compression tests will provide microstructural evolution information. The Johnson-Cook and Zerilli-Armstrong models are commonly used in the deformation processing and armor materials literature to compare mechanical properties at elevated temperatures and strain rates.

Plans for Next Reporting Period

Avenues of investigation for the next reporting period include:

- Microstructural and mechanical characterization of ATI baseline material, including the as-received state and after Gleeble deformation;
- Complete composition selection of iron-containing MPEAs;
- Initial melting of candidate MPEA samples in the arc melter at Mines.

References

[55.1] Y.F. Ye, Q. Wang, J. Lu, C.T. Liu, Y. Yang, High-Entropy Alloys: Challenges and Prospects, Materials Today. 19(6) (2016) 349-362.

[55.2] R.S. Mishra, R.S. Haridas, P. Agrawal, High Entropy Alloys – Tunability of Deformation Mechanisms Through Integration of Compositional and Microstructural Domains, Mater. Sci. Eng. A. 812 (2021) 141085.

[55.3] P. Hazell, Armour Materials, Theory, and Design, CRC Press (2015).

[55.4] A. Saxena, A. Kumaraswamy, N. Kotkunde, K. Suresh, Constitutive Modeling of High-Temperature Flow Stress of Armor Steel in Ballistic Applications: A Comparative Study, J. Mater. Eng. Perform 28 (2019) 6505–6513.

[55.5] J. Copley, F.G. Coury, B. Ellyson, A.J. Clarke, Identification Of TRIP Alloys By CALPHAD Methods, An Accessible Approach (preprint), (n.d.).

[55.6] F.G. Coury, K.D. Clarke, C.S. Kiminami, M.J. Kaufman, A.J. Clarke, High Throughput Discovery and Design of Strong Multicomponent Metallic Solid Solutions, Sci. Rep. 8 (2018) 1–10.

[55.7] Z. Li, C.C. Tasan, K.G. Pradeep, D. Raabe, A TRIP-Assisted Dual-Phase High-Entropy Alloy: Grain Size and Phase Fraction Effects on Deformation Behavior, Acta Mater. 131 (2017) 323–335.

[55.8] Y.L. Zhao, T. Yang, J.H. Zhu, D. Chen, Y. Yang, A. Hu, C.T. Liu, J.-J. Kai, Development Of High-Strength Co-Free High-Entropy Alloys Hardened By Nanosized Precipitates, Scripta Mater. 148 (2018) 51-55.

[55.9] N.J. Wengrenovich, The Optimization and Design of a Fully Austenitic, Gamma-Prime Strengthened TRIP Steel for Blast and Fragment Resistance, Ph.D dissertation, Northwestern University, 2016.

[55.10] F. Haftlang, P. Asghari-Rad, J. Moon, A. Zargaran, K.-A. Lee, S.-J. Hong, H.S. Kim, "Simultaneous Effects of Deformation-Induced Plasticity and Precipitation Hardening in Metastable Non-Equiatomic FeNiCoMnNiTiSi Ferrous Medium-Entropy Alloy at Room and Liquid Nitrogen Temperatures, Scripta Mater. 202 (2021) 114013.

[55.11] S. Curtze, V.T. Kuokkala, Dependence of Tensile Deformation Behavior of TWIP Steels on Stacking Fault Energy, Temperature and Strain Rate, Acta Mater 58 (2010) 5129–41.

[55.12] S. Curtze, V.T. Kuokkala, A. Oikari, J. Talonen, H. Hänninen, Thermodynamic Modeling Of The Stacking Fault Energy Of Austenitic Steels, Acta Mater. 59 (2011) 1068–1076.

55.5 Figures and Tables

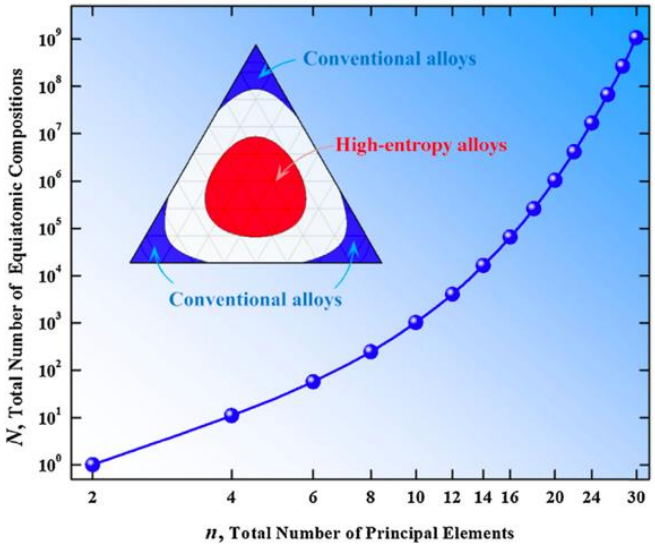

Figure 55.1: A visual representation of the MPEA design concept, from [55.1]

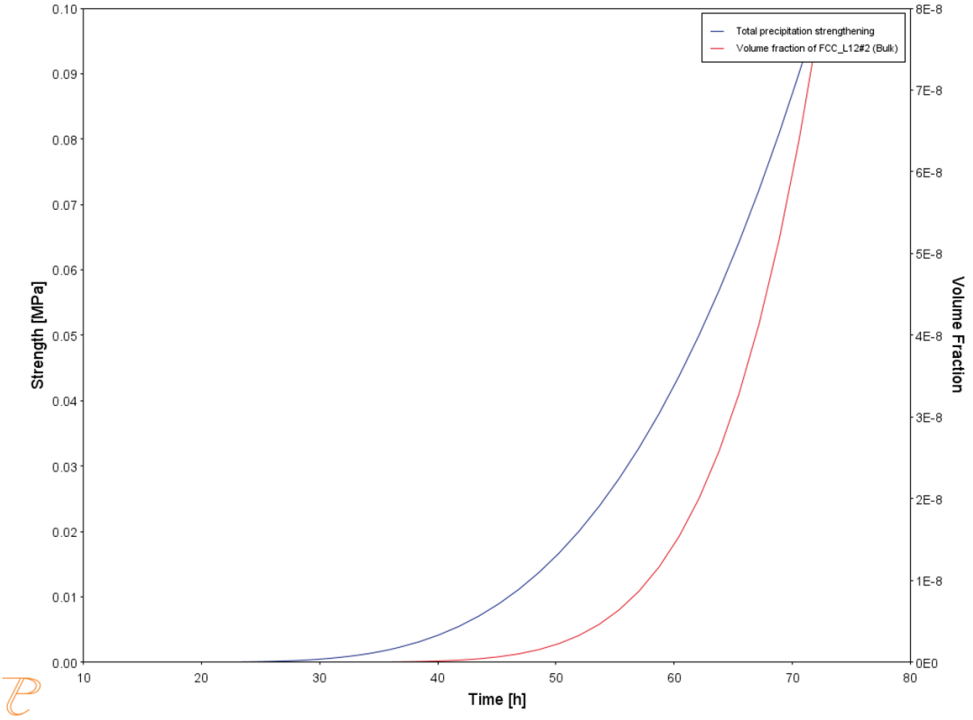

Figure 55.2: Isothermal transformation curve for $Fe_{58}Ni_{25}Al_{10}Mn_8Ti_4C_{2.4}$ at T = 330°C.

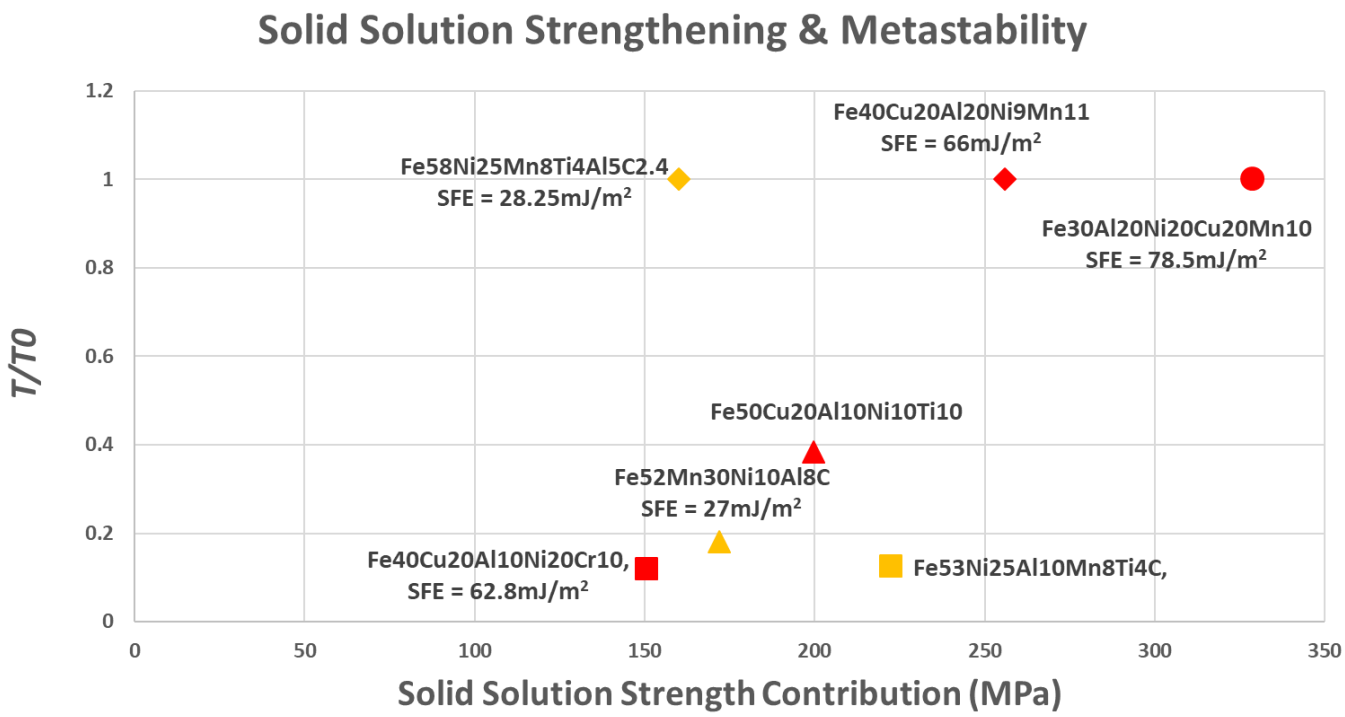

Figure 55.3: T/T_0 TRIP susceptibility parameter plotted against TC-EARS solid solution contribution for six candidate compositions.

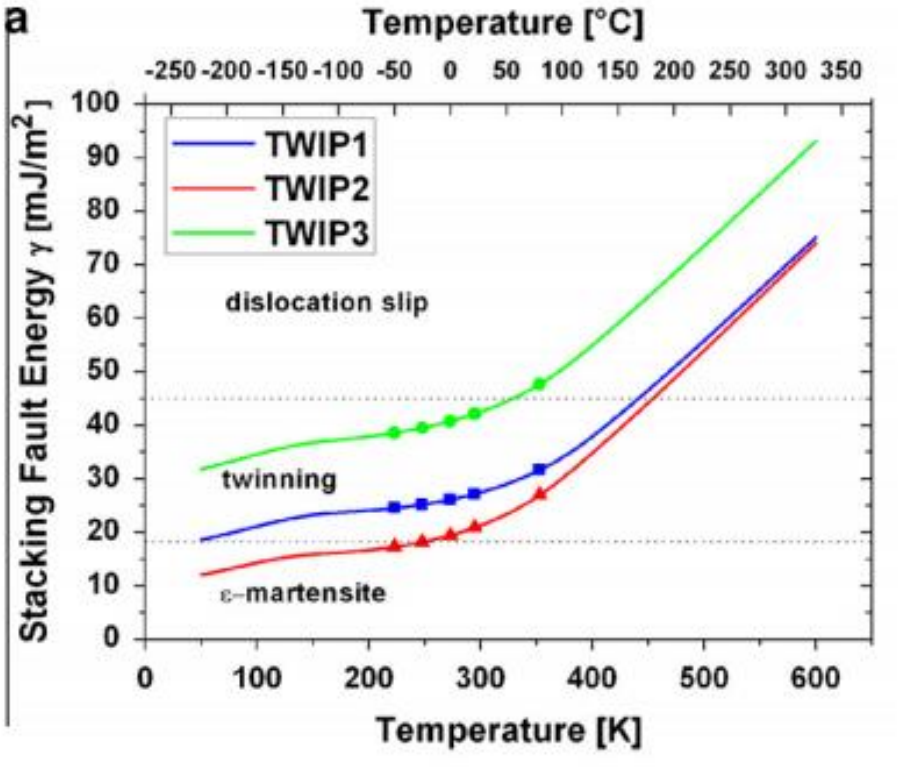

Figure 55.4: Relationship of deformation mechanism to stacking fault energy. From [55.11]

T (°C)	Room Temp	Medium	Peak Impact Temperature
Strain rate (s^-1)			
Quasistatic (10^-3)	Tensile	Gleeble Tensile	Gleeble Tensile
High (~100) -- Mid -- Low (10^-2)	Tensile	Gleeble Tensile	Gleeble Tensile
	Tensile	Gleeble Tensile	Gleeble Tensile

Figure 55.5: Mechanical test matrix for tensile specimens. Note that peak impact temperature is approx. 1000°C.

T (°C)	Room Temp	Warm Work Temperature	Hot Work/Supersolvus
Strain rate (s^-1)			
Quasistatic (10^-3)	Gleeble Compression	Gleeble Compression	Gleeble Compression
High (~100) -- Mid -- Low (10^-2)	Gleeble Compression	Gleeble Compression	Gleeble Compression
		Gleeble Compression	Gleeble Compression

Figure 55.6: Mechanical test matrix for compression specimens. Note that supersolvus temperature is approx. 1100°C for γ' strengthened alloys. The high strain rate room temperature condition is excluded here because of the likelihood of cracking.